Cofactor-Directed Reversible Denaturation Pathways: The Cofactor-Stabilized *Escherichia coli* Aspartate Aminotransferase Homodimer Unfolds through a Pathway That Differs from That of the Apoenzyme†

Edgar Deu and Jack F. Kirsch*

Department of Molecular and Cell Biology, University of California, Berkeley, Berkeley, California 94720-3206

Received December 21, 2006; Revised Manuscript Received March 7, 2007

ABSTRACT: While the urea-mediated unfolding pathway of the *Escherichia coli* aspartate aminotransferase (eAATase) homodimer proceeds through a reversible three-state process with a partially folded dimeric intermediate, D ⇄ D* ⇄ 2U (E. Deu and J. F. Kirsch, accompanying paper), that of a cofactor-stabilized form differs. Pyridoxal phosphate, which binds at the intersubunit active sites, stabilizes the native form by 6 kcal mol^{-1} and dissociates during the D ⇄ D* transition. Reductive trapping of the cofactor to a nondissociable derivative (PPL-eAATase) precludes the formation of D*. A novel monomeric intermediate (M′-PPL) with 70% of the native secondary structure (circular dichroism) was identified in the unfolding pathway of PPL-eAATase: D-PPL$_2$ ⇄ 2M′-PPL ⇄ 2U-PPL. The combined results define two structural regions with distinct stabilities: the active site region (ASR) and the generally more stable, dimerization region (DMR). The DMR includes the key intersubunit contacts. It is responsible for the multimeric nature of D*, and its disorder leads to dimer dissociation. Selective strengthening of the ASR−cofactor interactions by cofactor trapping reverses the relative stabilities of the two regions (from DMR > ASR in the apoenzyme to ASR > DMR in PPL-eAATase) and results in a reordering of the eAATase denaturation pathway.

Although more than 30% of all proteins require cofactors for biological function, their roles in protein stability and folding have been relatively unexplored (*1*). In addition to helping to stabilize the native forms (*2*−*6*), they have been reported to have active roles in protein folding. In some cases, they bind to the unfolded states (*3*, *5*, *7*, *8*) and accelerate the folding reaction (*7*, *8*), or they guide the polypeptide chains to the correct conformations (*7*, *8*). In other instances, they associate only with partially folded states (*3*, *9*) or with the native forms (*4*) and stabilize the latter by decreasing the unfolding rates (*4*, *5*).

Large oligomeric proteins are generally composed of several domains and may contain multiple cofactors. The formation of multidomain proteins is thought to proceed through the independent folding of each domain prior to assembly into functional structures (*10*). Proteins containing domains of different stability often present several cooperative unfolding transitions, one per domain, at distinct melting temperatures, pH values, or denaturant concentrations (*11*−*13*). Oligomeric complexes can be considered as multidomain entities whose intra- and/or interchain domains are not all connected through the peptide backbone.

The effect of cofactors on the stability of multimeric proteins will depend on location. They might exclusively stabilize a cofactor binding domain or increase the compactness of the native form by mediating interactions across domains (*2*). If nested at the subunit interface of oligomers, they will probably be important for quaternary structure formation (*9*) or might consolidate intersubunit domains.

The pyridoxal 5′-phosphate (PLP)[1] dependent homodimer (87 kDa) *Escherichia coli* aspartate aminotransferase (eAATase) provides a flexible system to study the contribution of cofactors to the stability of large multimeric proteins. This enzyme has been thoroughly characterized by chemical denaturation studies (*14*−*17*). The holo form is significantly more stable than the apo form in *E. coli* (*14*), as well as in mitochondrial (*18*, *19*) and cytosolic (*20*) aspartate aminotransferases. The accompanying paper (E. Deu and J. F. Kirsch, accompanying paper) describes a partially folded dimeric intermediate, D*, in the urea-mediated unfolding pathway of apo-eAATase (eq 1):

$$\mathrm{D} \rightleftarrows \mathrm{D}^* \rightleftarrows 2\mathrm{U} \qquad (1)$$

where D is the native apoenzyme and U the unfolded state. D* is very stable ($\Delta G^0_{\mathrm{D}^* \rightleftarrows 2\mathrm{U}}$ = 24.4 kcal mol^{-1}), unfolds

† This work was supported NIH Grant GM 35393.

* To whom correspondence should be addressed. Telephone: (510) 642-6368. Fax: (510) 642-6368. E-mail: jfkirsch@berkeley.edu.

[1] Abbreviations: ΔASA, change in accessible surface area; $\Delta G^0_{\mathrm{unf}}$, free energy of unfolding at 0 M denaturant; θ_{N}, normalized ellipticity signal; ASR, active site region; C_{m}, denaturant concentration at a transition midpoint; D, native dimeric state; D*, partially folded dimeric intermediate; DMR, dimerization region; DTT, dithiothreitol; eAATase, *Escherichia coli* aspartate aminotransferase; Fl, fluorescence; F_{N}, normalized fluorescence emission; His_6 tag, 6-histidine tag; GdnHCl, guanidine hydrochloride; I, partially folded intermediate; IAEW, intensity-averaged emission wavelength; M′-PPL, partially folded monomeric intermediate in the denaturation of PPL-eAATase; MDH, malate dehydrogenase; N, native state; PLP, pyridoxal 5′-phosphate; PMP, pyridoxamine 5′-phosphate; PPL, phosphopyridoxyllysyl; TAPS, *N*-[tris(hydroxymethyl)methyl]-3-aminopropanesulfonic acid; U, unfolded state.

10.1021/bi602632d CCC: $37.00
Published on Web 04/19/2007

cooperatively, and retains 40% of the native secondary structure (circular dichroism). The strong cooperativities of the D ⇄ D* and D* ⇄ 2U transitions reveal two structural regions with distinct stabilities.

eAATase catalyzes the reversible transfer of an amino group from an acidic amino acid to the α-carbon of a dicarboxylic keto acid according to the ping-pong mechanism of eqs 2 and 3 (*21*, *22*):

$$\text{L-aspartate} + \text{E}-\text{PLP} \rightleftarrows \text{oxaloacetate} + \text{E}-\text{PMP} \quad (2)$$

$$\text{E}-\text{PMP} + \alpha\text{-ketoglutarate} \rightleftarrows \text{E}-\text{PLP} + \text{L-glutamate} \quad (3)$$

where E−PLP and E−PMP correspond to the covalently bound PLP−enzyme (PLP-eAATase or PLP form) and the noncovalently bound pyridoxamine phosphate (PMP)−enzyme (PMP-eAATase or PMP form) complexes, respectively. PLP forms an imine with Lys258.

The dissociation constants for PLP and PMP forms are 0.4 ± 0.2 pM and 1.28 ± 0.03 nM, respectively (*23*). Several crystal structures of both holoenzymes are available (*24*−*27*). They show that the cofactors mediate inter- and intrasubunit contacts. Additionally, the contributions of specific interactions to cofactor binding and catalysis have been evaluated by site-directed mutagenesis (*23*, *28*−*50*).

The eAATase active site provides a favorable degree of flexibility to study the effects of cofactor association on stability. Several folded forms of the enzyme that differ only in the occupant of the cofactor binding site are easily prepared. Four species, with increasing favorable enzyme−cofactor interactions, apo, PMP, PLP, and reduced forms, were compared in this work. The last specie is obtained by reduction of the above-mentioned Schiff base to phosphopyridoxyllysine (PPL) to yield a covalently trapped PLP derivative that is retained in the denatured enzyme.

In this investigation, the cofactor contributions to the stability of eAATase confirmed (E. Deu and J. F. Kirsch, accompanying paper) the presence of two structural regions, which are here delineated into the active site region (ASR) and the dimerization region (DMR). Strengthening the enzyme−cofactor interactions inverts the relative stabilities of these two regions, as well as the order of the urea-mediated denaturation steps.

MATERIALS AND METHODS

Preparation of the PLP, PMP, and Reduced Forms of eAATase. The PLP form was prepared as previously described (*49*, *51*) (E. Deu and J. F. Kirsch, accompanying paper). The PMP form was obtained by incubating 100 μM PLP-eAATase in buffer A (20 mM potassium phosphate, pH 7.5, and 1 mM DTT) containing 100 μM PMP and 70 mM L-Asp for 30 min at room temperature. The extent of conversion of the PLP to the PMP form was monitored by absorbance. Only the single 330 nm absorbance cofactor band characteristic of the PMP form was present.

Reduction of the Lys258-PLP Schiff base is described in ref *49*. Holoenzyme (50−100 μM) was incubated for 10 min at room temperature in 20 mM potassium phosphate, 20 μM PLP, and 35 mM oxaloacetate at pH 7.5. A solution of 0.5 M $NaCNBH_4$ (in 0.05 M NaOH) was added to a final concentration of 40 mM, and the mixture was kept for 30 min at 25 °C. Oxaloacetate and excess reducing agent were dialyzed out against 20 mM potassium phosphate, pH 7.5, and 4 °C. The absorbance spectrum and residual activity of the reduced form (PPL-eAATase or PPL form) showed that >95% of the Lys258-PLP Schiff base was reduced to PPL.

Equilibrium Denaturation and Renaturation of eAATase. eAATase samples (0.1−10 μM) were incubated overnight at room temperature in buffer A containing selected concentrations of urea or guanidine hydrochloride (GdnHCl). The respective cofactors were added to 10 μM concentration to buffer A for the study of the PLP or PMP forms. Samples were kept in the dark to prevent photobleaching of the cofactor. All measurements were taken at 25 °C. The renaturation experiments from the unfolded state were performed as described in the accompanying paper (E. Deu and J. F. Kirsch, accompanying paper) but with the addition of 10 μM pertinent cofactor. The same procedure was followed to reconstitute partially denatured protein that was incubated for 3 h at 25 °C in 4.5 M urea.

Activity as a Function of Denaturant Concentration. The residual activity following overnight incubation with denaturant was assessed by diluting an aliquot of the equilibrated samples into assay buffer (200 mM TAPS−KOH, 100 mM KCl, 150 μM NADH, 8 units/mL malate dehydrogenase (MDH), 20 mM L-Asp, and 6 mM α-ketoglutarate at pH 8.4) and measuring the initial activity with the MDH coupled assay (*21*, *52*). The decrease in NADH concentration at 340 nm was monitored on a Perkin-Elmer Lambda 4B spectrophotometer. PLP was omitted to minimize reconstitution of holoenzyme. No increase in activity was observed during the time of the assay. Control experiments showed that the residual denaturant has no effect on the rates of the MDH coupled reactions.

Effect of Cofactor Concentration on the Denaturant-Mediated Inactivation of PLP-eAATase. PLP-eAATase (0.1 μM) was incubated overnight at room temperature in buffer A containing selected concentrations of either urea or GdnHCl and 0.1−10 μM PLP. The residual activity at each denaturant and cofactor concentration was measured as described above on a Molecular Devices Spectra MAX 190 plate-reader spectrophotometer.

Spectrophotometric Measurements. (A) Fluorescence. Tryptophan emission was recorded from 300 to 400 nm (λ_{ex} = 280 nm). The emission intensity at 335 nm was chosen to monitor the unfolding of all eAATase species. Emission measurements at 393 and 395 nm (λ_{ex} = 330 nm) (*53*) were employed to monitor selectively the environment surrounding the cofactor in the PMP and PPL forms, respectively. Intensity-averaged emission wavelengths (IAEW) were computed from the emission spectra as indicated in E. Deu and J. F. Kirsch (accompanying paper). All measurements were done on a Perkin-Elmer LB50S fluorometer at 25 °C.

(B) Circular Dichroism. All CD measurements were taken on an Aviv 62DS spectrometer at 25 °C. PLP- or PPL-eAATase spectra were recorded from 190 to 260 nm. The ellipticity values were calculated as the average over 1 s nm^{-1}. Cuvettes of 1 and 0.1 cm path length were used for samples containing 0.5 and 10 μM enzyme, respectively (E. Deu and J. F. Kirsch, accompanying paper). The molar ellipticity at 222 nm (θ_{222}) was chosen to monitor the loss of secondary structure.

Reductive Trapping of PLP to the Enzyme. The residual PLP bound to Lys258 was trapped by adding 5 μL of 1 M $NaCNBH_4$ (in 0.05 M NaOH) to 100 μL of preequilibrated samples that contained 10 μM PLP-eAATase, 10 μM PLP, and selected denaturant concentrations in buffer A. After 30 min at room temperature, each sample was diluted 10-fold into 8.5 M urea and incubated for 1 h to ensure complete unfolding. The fluorescence properties of PPL were used to quantify the fraction of enzyme-associated cofactor at each denaturant concentration.

Data Analysis. All C_m values were obtained by fitting the data to unimolecular denaturation models based on the linear extrapolation method (*54*, *55*). The data were fit with KaleidaGraph to a two-state model (eq 4) with eq 5 (*56*) when the probe showed evidence for a single denaturation step:

$$N \rightleftarrows U \quad (4)$$

$$S = [({S_N}^0 + \alpha_N[\mathrm{Den}]) + ({S_U}^0 + \alpha_U[\mathrm{Den}])K_{N\rightleftarrows U}]/(1 + K_{N\rightleftarrows U}) \quad (5)$$

where N and U are the native and unfolded states, respectively; $K_{N\rightleftarrows U} = \exp[m_{N\rightleftarrows U}([\mathrm{Den}] - C_{m,N\rightleftarrows U})/RT]$; S is the measured signal; ${S_i}^0$, the intrinsic signal of species i at 0 M denaturant; α_i, the dependence of the intrinsic signal of species i on denaturant concentration; [Den], the denaturant concentration; and m, the cooperativity parameter for the indexed equilibrium process.

Data consistent with a three-state model (eq 6) were fitted to eq 7 (*57*, *58*) using the KaleidaGraph program:

$$N \rightleftarrows I \rightleftarrows U \quad (6)$$

$$S = [({S_N}^0 + \alpha_N[\mathrm{Den}]) + {S_I}^0 K_{N\rightleftarrows I} + ({S_U}^0 + \alpha_U[\mathrm{Den}])K_{N\rightleftarrows I}K_{N\rightleftarrows U}]/[1 + K_{N\rightleftarrows I}(1 + K_{N\rightleftarrows U})] \quad (7)$$

where I is a partially folded species; $K_{N\rightleftarrows I} = \exp[m_{N\rightleftarrows I}([\mathrm{Den}] - C_{m,N\rightleftarrows I})/RT]$ and $K_{I\rightleftarrows U} = \exp[m_{I\rightleftarrows U}([\mathrm{Den}] - C_{m,I\rightleftarrows U})/RT]$. The term α_I was omitted from eq 7 because of the absence of an intermediate signal baseline. Equations 5 and 7 are more fully described in E. Deu and J. F. Kirsch (accompanying paper). The data collected for the PMP or PLP forms were globally fitted to a three-state model including a dimeric intermediate (eq 1) using the formalism described for the apo form (E. Deu and J. F. Kirsch, accompanying paper) and the SAS statistical package (SAS Institute, Cary, NC).

RESULTS

Urea-Mediated Denaturation of PLP-eAATase. (A) Loss of Activity and PLP Dissociation. The observed decrease in catalytic activity (Figure 1) of eAATase with increasing concentrations of denaturant can be due only to cofactor release, dimer dissociation, or alteration of the active site. The inactivation curves are enzyme concentration independent; thus the loss of activity is not due to dimer dissociation. All inactivation C_m values (Table 1) are identical within experimental error and are comparable to those reported by Gloss et al. (*59*) under similar experimental conditions.

The inset in Figure 1 shows that cofactor dissociation from 10 μM holoenzyme follows the same dependence on denaturant as does the loss of activity. (See Table 1 for C_m values.) Enzyme inactivation is thus due to cofactor dissociation. The reaction was further investigated by CD and fluorescence in order to discover if PLP release is accompanied by an observable conformational change (see below).

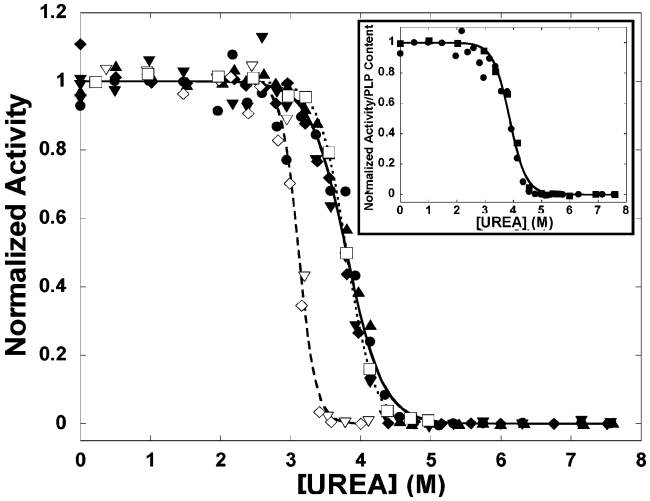

FIGURE 1: Dependence of PLP-eAATase activity and extent of PLP dissociation on urea concentration. Native (solid symbols), partially unfolded (□), or unfolded (open symbols except □) forms of the enzyme were diluted to final concentrations of 0.1 (▼, ▽), 0.5 (◆, ◇, □), 2.5 (▲), and 10 μM (●) into 0−8 M urea in buffer A containing 10 μM PLP and incubated overnight at 25 °C. The partially unfolded and unfolded forms of the enzyme used for the refolding experiments were obtained by incubating the enzyme in 4.5 M urea for 3 h (less than 40% of the enzyme was active) or in 7 M urea for 30 min, respectively. The residual activities were measured with the MDH coupled assay. Inset: The extent of PLP dissociation from 10 μM samples (■) was measured after reduction of the Lys258-PLP Schiff base to PPL followed by complete denaturation of the protein (see Materials and Methods). Bound PPL was quantified by fluorescence (λ_{ex} = 330 nm, λ_{em} = 395 nm). The lines correspond to the fit of the unfolding (solid lines) and refolding (discontinuous lines) data to a simple two-state denaturation model (eq 5).

Reversibility of the Denaturation Process. The recovery of activity during refolding from U takes place at lower urea concentrations than does enzyme inactivation (Figure 1). More than 70% of the native activity is recovered. Interestingly, the reactivation curves are enzyme concentration independent (Table 1). Although the observation of hysteresis might indicate that equilibrium is not reached in the transition region under the employed experimental conditions, the unfolding and refolding curves of PPL- (see below) and apo-eAATases (E. Deu and J. F. Kirsch, accompanying paper) are superimposable. Moreover, the recovery of activity of partially unfolded enzyme that retains less than 40% of its activity is coincident with the inactivation curves (Figure 1), therefore proving that equilibrium has been established. (See Discussion for possible explanation of the observed hysteresis.)

(*B*) *Fluorescence.* The dependences of PLP-eAATase emission properties as functions of urea and enzyme concentrations are shown in Figure 2. Two denaturation processes characterized by an increase and a decrease in emission intensity, as well as IAEW shifts initially from 342 to 345 nm and further to 348 nm, clearly show the presence of an unfolding intermediate. The fitted C_m values of the low urea concentration transition are independent of enzyme

Table 1: C_m Values Describing the Denaturation of Holo-eAATases[a]

PLP Form				
denaturant	probe	[enzyme] (μM)	$C_{m,D-PLP_2 \rightleftarrows D^*}$ (M)	$C_{m,D^* \rightleftarrows 2U}$ (M)
urea	Fl (335 nm)	0.5	4.05 (0.03)	4.37 (0.09)
	Fl (335 nm)	2.5	3.94 (0.02)	4.86 (0.04)
	Fl (335 nm)	10	3.89 (0.04)	5.02 (0.03)
	Fl (335 nm)	10[b]	3.5 (0.2)	5.10 (0.04)
	CD (222 nm)	0.5	3.62 (0.08)	4.3 (0.6)
	CD (222 nm)	10	3.84 (0.03)	5.17 (0.03)
	activity	0.1	3.71 (0.03)	–
	activity	0.1[b]	3.16 (0.01)	–
	activity	0.5	3.77 (0.02)	–
	activity	0.5[b]	3.08 (0.02)	–
	activity	2.5	3.86 (0.02)	–
	activity	10	3.94 (0.04)	–
	PLP dissociation	10	4.01 (0.03)	–
	average	–	3.9 (0.2)	–
GdnHCl	Fl (IAEW)	0.5	1.04 (0.05)	1.84 (0.07)
	Fl (IAEW)	10	1.12 (0.01)	2.19 (0.04)
	activity	0.5	1.06 (0.03)	–
	activity	10	1.11 (0.01)	–
	PLP dissociation	10	1.06 (0.03)	–
	average	–	1.09 (0.05)	–
	PLP dissociation[c]	0.1[d]	0.77 (0.01)	–
		0.2[d]	0.93 (0.01)	–
		1.0[d]	1.02 (0.01)	–
		10[d]	1.11 (0.02)	–
PMP Form				
denaturant	probe	[enzyme] (μM)	$C_{m,D-PMP_2 \rightleftarrows D^*}$ (M)	$C_{m,D^* \rightleftarrows 2U}$ (M)
urea	Fl (335 nm)	10	3.01 (0.03)	5.12 (0.05)
	Fl (335 nm)	10[b]	2.58 (0.04)	5.28 (0.02)
	Fl (393 nm)	10	2.96 (0.03)	–
	activity	1	3.3 (0.04)	–
	activity	1[b]	2.5 (0.05)	–
	average	–	3.1 (0.2)	–

[a] The C_m values for the subscripted transitions are reported for the different probes: fluorescence (Fl), monitoring either the changes in PMP (393 nm) or tryptophan emission (335 nm or IAEW), CD, activity, and PLP dissociation. Equations 5 or 7 were used for probes presenting one or two denaturation transitions, respectively. Average values are for the denaturation data only. [b] Renaturation experiments. [c] 0.1 μM PLP-eAATase. [d] [Enzyme] = [PLP].

concentration within experimental error and correspond to those obtained from the inactivation and PLP dissociation curves (Table 1). An increase in emission intensity is expected upon cofactor release since apo-eAATase has a much higher quantum yield than the holo forms (*18*). However, the intermediate λ_{max} (345 nm) is significantly red shifted from that of the native apo form (337 nm) (E. Deu and J. F. Kirsch, accompanying paper), which denotes a higher degree of solvent exposure of the aromatic residues, and indicates that a conformational change accompanies PLP dissociation during unfolding.

The second transition is enzyme concentration dependent and therefore corresponds to dimer dissociation. The observed concentration dependence of the first transition is due to the coupled contribution from the dissociation process, which is especially manifested at low enzyme concentrations. The relative enhancement in emission intensity at 4.5 M urea with increasing monomer concentration is consistent with

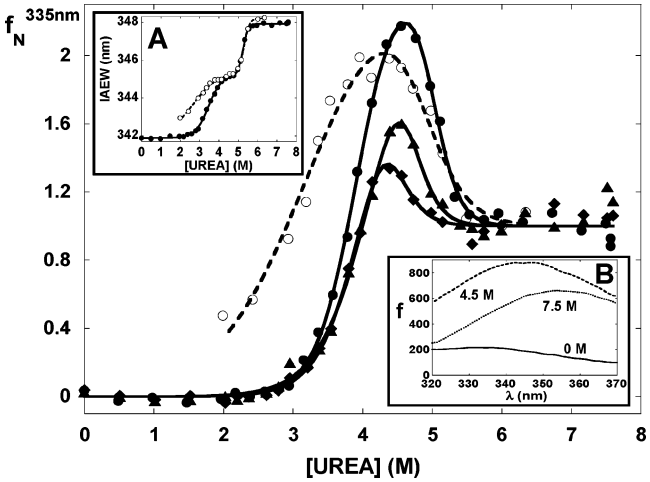

FIGURE 2: PLP-eAATase fluorescence as a function of urea concentration. Samples were incubated overnight at 25 °C in buffer A containing 0−8 M urea and 10 μM PLP. Emission spectra were recorded from 300 to 400 nm (λ_{ex} = 280 nm). The changes in emission at 335 nm and in IAEW (inset A) are shown for 0.5 (◆), 2.5 (▲), and 10 μM (●) enzyme. The refolding of 10 μM eAATase (○) was performed as described in Materials and Methods. The emission spectra of samples containing 10 μM enzyme at the indicated urea concentrations are shown in inset B. The fits of the denaturation and renaturation data to eq 7 are represented by solid and dashed lines, respectively (main panel and inset A).

the accumulation of a dimeric intermediate. The IAEW red shift and the >2-fold decrease in emission intensity observed in the second transition at 10 μM PLP-eAATase are equivalent to those observed for the denaturation of the apo form under the same conditions (E. Deu and J. F. Kirsch, accompanying paper). Therefore, the denaturation of PLP-eAATase is a two-step process involving initial PLP dissociation with formation of a dimeric intermediate, followed by the dissociation to unfolded monomers.

The renaturation curve at 10 μM enzyme presents hysteresis behavior for the PLP dissociation step, consistent with that observed in the reactivation curves (Figure 1). The dimer ⇄ monomers process reaches equilibrium under the above-described experimental conditions (Figure 2 and Table 1).

(*C) Circular Dichroism.* The changes in ellipticity at 222 nm (θ_{222}) of PLP-eAATase samples as a function of increasing urea concentration also show formation of an intermediate at ca. 4.5 M urea (Figure 3). The second transition is enzyme concentration dependent, and the C_m values associated with those curves are consistent with the results described above (Table 1). The θ_{222} values indicate that the intermediate retains 40% of the native secondary structure as was shown for the apo form (E. Deu and J. F. Kirsch, accompanying paper).

The dimeric intermediates formed in the unfolding of apo- and PLP-eAATases have the same spectrophotometric properties, and their denaturation curves are superimposable above 4.5 M urea. (See Discussion section.) These observations demonstrate that the partially folded species observed in the urea-mediated denaturation of those forms is the same intermediate. The denaturation of PLP-eAATase can thus be described by the following equilibrium model (eq 8):

$$\text{D-PLP}_2 \rightleftarrows 2\text{PLP} + \text{D}^* \rightleftarrows 2\text{U} \qquad (8)$$

GdnHCl-Promoted Denaturation of PLP-eAATase. The data in the accompanying paper (E. Deu and J. F. Kirsch,

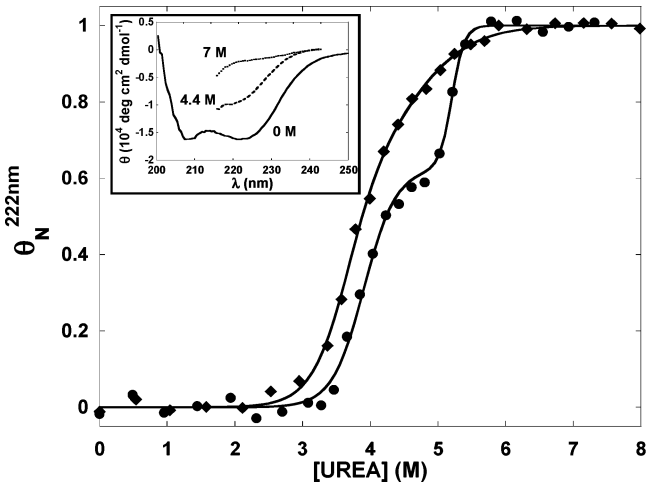

FIGURE 3: Molar ellipticity of PLP-eAATase in urea. The normalized θ_{222} of 0.5 (◆) and 10 μM (●) PLP-eAATase samples following overnight incubation at 25 °C in 0−8 M urea and 10 μM PLP (buffer A) are shown. The data were fitted to eq 7. The inset shows the CD spectra of 10 μM enzymes at the noted urea concentrations.

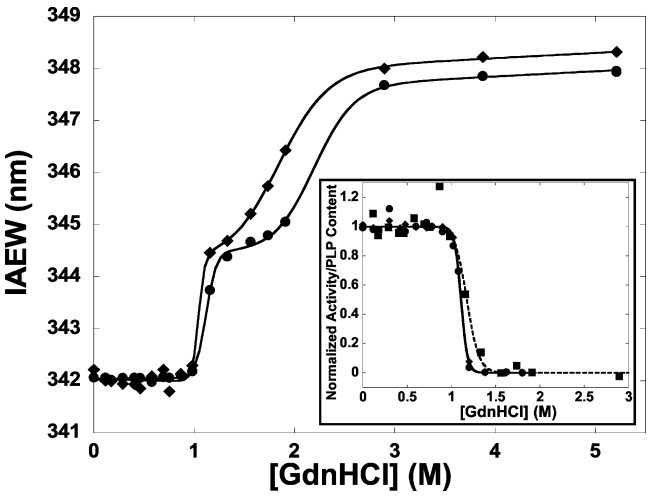

FIGURE 4: Dependence of PLP-eAATase fluorescence, activity, and cofactor dissociation on GdnHCl concentration. The denaturation of 0.5 (◆) and 10 μM (●) enzyme in GdnHCl was monitored by IAEW (λ_{ex} = 280 nm) and residual activity (inset). Samples containing 0−5.2 M GdnHCl in buffer A were incubated overnight at 25 °C before data collection. The extent of PLP dissociation at 10 μM enzyme (■) was measured by chemical cross-linking as described in Materials and Methods. Equation 7 was used to fit the IAEW values and eq 5 for the activity and PLP dissociation (dashed line) data.

accompanying paper) show that the unfolding pathway of apo-eAATase depends on the structure of the denaturant. Apo-eAATase unfolds through a monomeric intermediate in GdnHCl (*14*) (eq 9), while D* is formed in urea. The

$$D \rightleftarrows 2M \rightleftarrows 2M^* \rightleftarrows 2U \quad (9)$$

effect of GdnHCl on the denaturation of the PLP form is presented here.

(*A) Fluorescence.* The shift in IAEW during the course of GdnHCl-mediated denaturation of PLP-eAATase also shows an enzyme concentration independent transition followed by one that is concentration dependent (Figure 4 and Table 1). Therefore, PLP-eAATase unfolds through a dimeric intermediate both in urea and in GdnHCl. Birolo et al. (*17*)

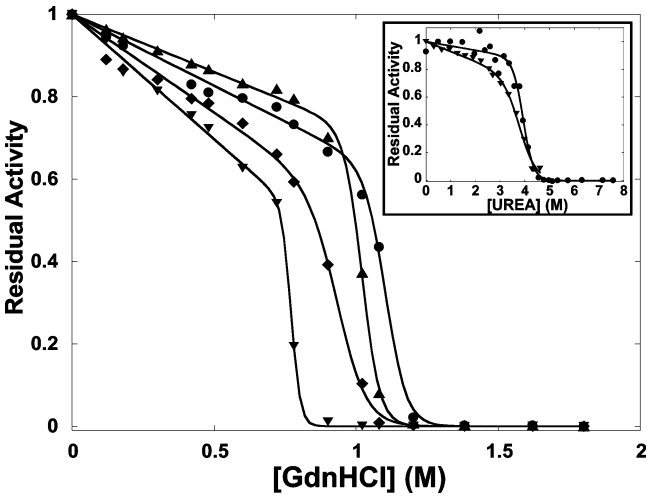

FIGURE 5: Dependence of the denaturant-mediated loss of eAATase activity on PLP concentration. 0.1 μM enzyme was incubated overnight at 25 °C at selected concentrations of GdnHCl or urea (inset) in buffer A containing a total of 0.1 (▼), 0.2 (◆), 1 (▲), and 10 μM (●) PLP. The residual activities of the samples were measured as described in Materials and Methods. The data sets were fitted to eq 5.

reported a very similar equilibrium denaturation curve (λ_{max} vs GdnHCl) at 1 μM PLP-eAATase. Although no dimeric intermediate was reported, the lower C_m value is within experimental error of those reported in Table 1. The higher one is between those reported here at 0.5 and 10 μM enzyme, which is consistent with a dimer dissociation process. Therefore, the intermediate described in ref *17* for a PLP-eAATase that lacks a C-terminal His_6 tag has similar properties to the one observed here.

(*B) Activity and PLP Dissociation.* The loss of activity in GdnHCl is also enzyme concentration independent, and the inactivation transition coincides with PLP dissociation (Figure 4, inset). These results appear to be at variance with those obtained in ref *14*, where the loss of activity in GdnHCl was reported to be dependent on enzyme concentration. The residual activities after overnight incubation at 25 °C of 0.1 μM PLP-eAATase at increasing concentrations of denaturant were monitored at selected cofactor concentrations (Figure 5). A decrease from 10 to 0.1 μM PLP lowers the inactivation C_m by more than 0.3 M GdnHCl (Table 1). A similar but less pronounced effect was observed in urea (Figure 5, inset). The independence of eAATase inactivation on protein concentration and its dependence on PLP content (Figures 1 and 5, respectively) clearly prove that the loss of activity is due to cofactor release and not dimer dissociation. The difference in results is likely due to the fact that PLP concentration was not controlled in ref *14*.

Denaturation of the PMP Form of eAATase. To better understand the stabilizing effect of the cofactor, the PMP form, which is not covalently attached to the enzyme, was studied by urea-mediated denaturation at 10 μM PMP-eAATase. The fluorescence properties of the PMP form under denaturation and renaturation conditions are presented in Figure 6, and the C_m values are reported in Table 1. The changes in tryptophan emission at 335 nm follow the same trend as those observed for the PLP form (Figure 2). The first transition (~3 M urea) occurs between those observed for the apo ($C_{m,D\rightleftarrows D^*}$ = 2.5 M) and PLP forms (Table 1) and is characterized by an increase of the PMP emission at 393

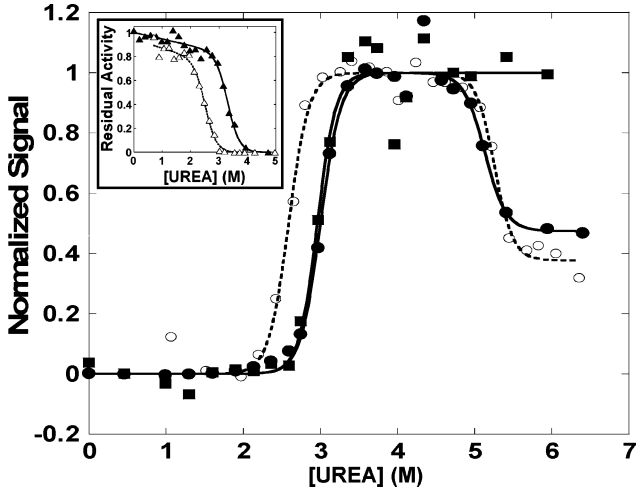

FIGURE 6: Dependence of PMP-eAATase fluorescence on urea concentration. All denaturation (solid symbols) and renaturation (open symbols) experiments were performed with 10 μM free PMP in buffer A. Tryptophan and PMP emissions were monitored at 335 (circles) and 393 nm (squares) (λ_{ex} = 280 and 330 nm), respectively, after overnight incubation at 10 μM PMP-eAATase and selected urea concentrations. The inset shows the change in residual activity (triangles) during denaturation and renaturation of 1 μM PMP-eAATase. Each unfolding (solid lines) and refolding (dashed lines) data set was fitted to eq 5 except that the tryptophan emission data were fitted to eq 7.

nm (λ_{ex} = 330 nm). No further changes in PMP fluorescence are observed at higher urea concentrations, demonstrating that the cofactor dissociates in the first transition. The second transition is identical to the D* $\rightleftarrows$ 2U step observed for the apo and PLP forms at the same enzyme concentration (E. Deu and J. F. Kirsch, accompanying paper). (See C_m values in Table 1.) All observations indicate that PMP-eAATase unfolds through the same dimeric intermediate as do the apo and PLP forms (eq 10) and that the more loosely bound PMP dissociates at lower urea concentration than does PLP.

$$\text{D-PMP}_2 \rightleftarrows 2\text{PMP} + \text{D}^* \rightleftarrows 2\text{U} \qquad (10)$$

The PMP form also displays hysteresis in the denaturation/refolding cycle (Figure 6). The D* $\rightleftarrows$ 2U process reaches equilibrium as seen for PLP-eAATase. Ninety percent of the activity is recovered in the renaturation of PMP-eAATase (Figure 6, inset), indicative of full reconstitution of the native enzyme.

Denaturation of the Reduced Form of eAATase (PPL-eAATase). (A) Circular Dichroism. To probe the contribution of the cofactor to enzyme stability further, it was irreversibly bound to the protein by cyanoborohydride reduction of the imine to a secondary amine. The loss of secondary structure of this form measured by θ_{222} in urea is shown in Figure 7. An intermediate that retains ca. 70% of the native secondary structure is present at 0.5 μM enzyme. Although this intermediate is not highly populated at 10 μM PPL-eAATase, the denaturation curve at that enzyme concentration fits better to a three-state (eq 7) than to a two-state model (eq 5). The curves and C_m values (last two rows of Table 2) clearly show that the transition at lower urea concentration is enzyme concentration dependent. The apparent shift of the second transition with protein concentration is probably due to the coupling of the two denaturation steps at 10 μM enzyme. Chemically cross-linking the cofactor to eAATase changes

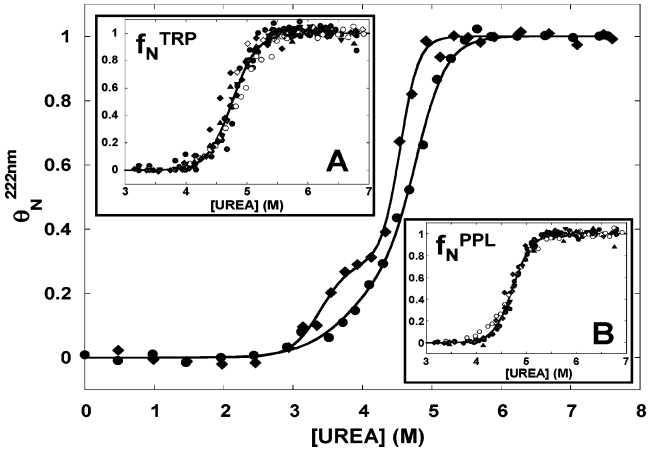

FIGURE 7: Effect of urea on the CD and fluorescence properties of the PPL-eAATase. 0.1 (▼), 0.5 (◆, ◇), 2.5 (▲), and 10 μM (●, ○) enzyme was incubated overnight at 25 °C in 0−8 M urea in buffer A lacking PLP. The normalized changes in θ_{222}, tryptophan emission (inset A; λ_{ex} = 280 nm, λ_{em} = 335 nm), and PPL emission (inset B; λ_{ex} = 330 nm, λ_{em} = 395 nm) during unfolding (solid symbols) and refolding (open symbols) are shown. The refolding experiments were performed by unfolding PPL-eAATase in 7 M urea for 30 min and incubating it in the indicated concentrations of urea. The fluorescence and CD data were fitted to eqs 5 and 7, respectively.

Table 2: C_m Values Describing the Denaturation of PPL-eAATase

probe	[enzyme] (μM)	$C_{m,D-PPL_2 \rightleftarrows 2M'-PPL}$ (M)	$C_{m,M'-PPL \rightleftarrows U-PPL}$ (M)
Fl (Trp)	0.1	−	4.76 (0.01)
Fl (Trp)	0.5	−	4.70 (0.02)
Fl (Trp)	2.5	−	4.67 (0.02)
Fl (Trp)	10	−	4.79 (0.01)
Fl (Trp)	10[a]	−	4.85 (0.01)
Fl (PPL)	0.1	−	4.75 (0.01)
Fl (PPL)	0.5	−	4.71 (0.01)
Fl (PPL)	2.5	−	4.73 (0.03)
Fl (PPL)	10	−	4.74 (0.01)
Fl (PPL)	10[a]	−	4.70 (0.01)
CD (222 nm)[b]	0.5	3.39 (0.08)	4.54 (0.02)
CD (222 nm)[b]	10[c]	3.88 (0.06)	4.78 (0.03)
average	−	−	4.73 (0.08)

[a] Renaturation experiment. [b] Obtained from eq 7. [c] S_I^0 was fixed at the value obtained from the CD data at 0.5 μM enzyme (0.30).

the unfolding mechanism from that of the apo (eq 1) and holo forms (eqs 8 and 10) to that given by eq 11:

$$\text{D-PPL}_2 \rightleftarrows 2\text{M}'\text{-PPL} \rightleftarrows 2\text{U-PPL} \qquad (11)$$

where D-PPL_2 represents the reduced form of the enzyme, M′-PPL a partially folded monomer, and U-PPL the PPL linked unfolded monomer.

(*B) Fluorescence.* The dependencies of tryptophan and PPL emission on urea concentration show only one transition that is enzyme concentration independent (Figure 7, insets). Its C_m values are similar to those obtained by CD for the M′-PPL $\rightleftarrows$ U-PPL process (Table 2). Surprisingly, no changes in fluorescence are observed upon dissociation of PPL-eAATase into monomers, even though the cofactor and Trp140 are at the subunit interface. The emission of the latter is largely quenched by the cofactor in the native PLP form (*18*). This might also be the case in M′-PPL, which would explain why the dissociation step is not signaled from the

changes in tryptophan emission. On the other hand, the cofactor must also be largely shielded from the solvent in M′-PPL as the PPL emission remains unchanged in the D-PPL_2 ⇄ 2M′-PPL transition. This is unexpected as a simple separation of the native dimer to folded monomer (M), based on the crystal structure, shows significant solvent exposure of the cofactor (*24*); therefore, M and M′-PPL must differ significantly in the structure contacting the cofactor.

DISCUSSION

Hysteresis in the Holo-eAATase Denaturation Cycle. While the urea-dependent denaturation curves for apo-eAATase are nearly superimposable upon those recorded for refolding (E. Deu and J. F. Kirsch, accompanying paper), hysteresis is observed in the D-PLP_2/PMP_2 ⇄ D* transition regions but not in the D* ⇄ 2U processes. The data were normalized; thus the hysteresis is not an artifact attributable to protein loss.

Hysteresis has been interpreted to indicate that the unfolding and folding processes are too slow to allow equilibrium to be established within the experimental incubation times (*60*−*63*). However, the extent of urea-mediated losses of activity and structure (measured by fluorescence) after 12, 24, or 48 h incubation are identical, which demonstrate that the D-PLP_2 ⇄ D* + 2PLP equilibrium was reached under the present experimental conditions (data not shown). Similarly, enzyme refolding, monitored with the same probes, reached a stationary point after 12 and 36 h incubation in 0−8 M urea (data not shown). Given these observations, the law of microscopic reversibility mandates that under these conditions the folding and unfolding mechanisms be different. Therefore, the observed hysteresis must reflect differences in the reacting species.

A possible explanation is that the 30 min exposure of the protein to 7 M urea prior to refolding leads to the formation of an alternate dimeric intermediate that is not identically capable of cofactor association as is D*. Possibilities include urea molecules occluded at the active site or denaturant-promoted tight association of phosphate at the cofactor binding site. This hypothesis is supported by the fact that no hysteresis is observed in the reconstitution of partially inactive enzyme obtained after 3 h incubation in 4.5 M urea (Figure 1). Cyanylation is an unlikely explanation as hysteresis was not observed for the apoenzyme (E. Deu and J. F. Kirsch, accompanying paper). In the denaturation experiments, the enzyme is not subjected to high urea concentrations prior to the formation of D*, and therefore that alternative intermediate is not observable.

Hysteresis is therefore due to the nonequivalence of the unfolding and refolding mechanisms. Equilibrium is established after overnight incubation of apo- and PPL-eAATases under both denaturating and renaturating conditions and of PLP-eAATase under the former conditions. Thus, free energies of unfolding can be obtained from the denaturation data of the holo forms.

*Apo-, PMP-, and PLP-eAATases Unfold through the Same Dimeric Intermediate, D**. As demonstrated above (Figures 1, 4, and 5), the cofactor dissociates upon D* formation. Further, the CD and fluorescence properties of D*, as well as the D* ⇄ 2U transitions, are identical for the three enzyme variants (Figure 8). D* is an extremely stable intermediate

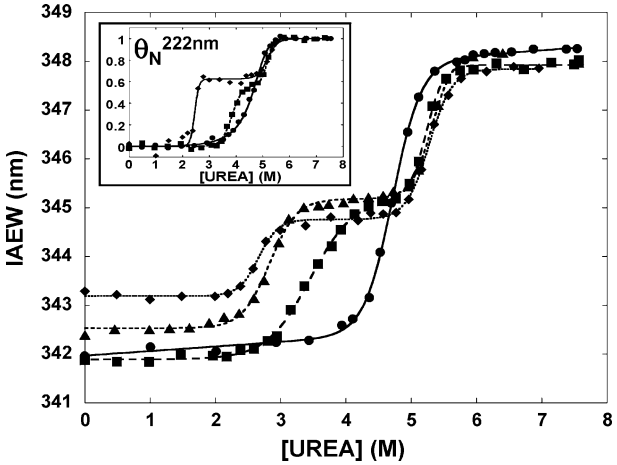

FIGURE 8: Effect of cofactor binding site occupancy on the stability of eAATase. The changes in IAEW and θ_{222} (inset) as a function of urea concentration are shown for 10 μM apo- (◆), PMP- (▲), PLP- (■), and reduced (●) eAATases. Each data set was fitted to eq 7. The data were collected after overnight incubation at 25 °C in buffer A containing 0−8 M urea and 10 μM appropriate cofactor for the holo forms.

Table 3: *m* and ΔG^0 Values Describing the Stability of eAATase Variants

	form			
	apo[a]	PMP[b]	PLP[c]	PPL
$\Delta G^0_{D\rightleftarrows D^*}$ (kcal mol^{-1})	12.2 (2.0)	13.6 (1.3)	18.3 (2.9)	
$m_{D\rightleftarrows D^*}$ (kcal mol^{-1} M^{-1})	4.8 (0.8)	4.6 (0.5)		
$\Delta G^0_{D^*\rightleftarrows 2U}$ (kcal mol^{-1})	24.4 (0.8)	28.3 (3.3)	24.4 (1.2)	
$m_{D^*\rightleftarrows 2U}$ (kcal mol^{-1} M^{-1})	3.4 (0.2)	4.2 (0.7)		
$\Delta G^0_{D-PPL_2\rightleftarrows 2M'-PPL}$ (kcal mol^{-1})				23.5 (0.9)[d]
$m_{D-PPL_2\rightleftarrows 2M'-PPL}$ (kcal mol^{-1} M^{-1})				4.4 (0.3)[d]
$\Delta G^0_{M'-PPL\rightleftarrows U-PPL}$ (kcal mol^{-1})				14.5 (0.4)[e]
$m_{M'-PPL\rightleftarrows U-PPL}$ (kcal mol^{-1} M^{-1})				3.1 (0.1)[e]

[a] From E. Deu and J. F. Kirsch (accompanying paper). [b] Only the data at 10 μM enzyme were fitted. [c] The apo-eAATase *m* values were used to yield these approximate ΔG^0 values. [d] Obtained from eqs 12−14 (Figure 9). [e] Obtained from eq 5.

($\Delta G^0_{D^*\rightleftarrows 2U} = 24 \pm 2$ kcal mol^{-1}; Table 3) and remains a dimer even when most of the native secondary structure is lost.

No monomeric intermediate is observed for the PLP form in the presence of GdnHCl (Figure 4), but one is seen for the apo form (E. Deu and J. F. Kirsch, accompanying paper) (*14*). The active site cofactor might impede access of guanidinium ions into the dimer interface, thus making M* kinetically inaccessible.

Effect of Active Site Stabilization on the Denaturation Pathway of eAATase. The native structure of AATase is stabilized by the cofactors (*14*, *19*, *20*). The stabilities of apo-, PMP-, PLP-, and PPL-eAATases are compared in Figure 8. The effect of the Schiff base is reflected in the greater stability of the PLP over the PMP form. As discussed above, D* formation necessitates cofactor release; therefore, it would be expected that locking the cofactor in place by

reduction (PPL form) should further stabilize D to the extent that a D*-PPL_2 species might be thermodynamically unstable. This expectation is realized in that a monomeric intermediate, M′-PPL, appears at low urea concentrations (Figure 7, eq 11). M′-PPL unfolds cooperatively and retains more secondary structure (70%) than the monomeric intermediate reported for the apo form at 1 M GdnHCl, M* (*14*). Additionally, its tryptophans and cofactor must still be shielded from the solvent since no change in the fluorescence of these chromophores is observed during the D-PPL_2 ⇄ 2M′-PPL transition.

Determination of the Free Energies of Unfolding for eAATase Variants. (A) Holo Forms. The PLP- and PMP-form data obtained from different probes were globally fitted to a D ⇄ D* ⇄ 2U denaturation model according to the formalism described in the accompanying paper (E. Deu and J. F. Kirsch, accompanying paper), which is based on the linear extrapolation method. As the native form of the enzyme is stabilized by the cofactors, the D-PLP_2/PMP_2 ⇄ D* transitions are shifted to higher urea concentrations compared with the apo form D ⇄ D* process (Figure 8). The D-PLP_2 ⇄ D* transitions cannot be fully resolved from the subsequent D* ⇄ 2U (Figures 2 and 3), thus precluding accurate determinations of the *m* and ΔG^0 parameters.

m values are generally accepted to be proportional to the change in solvent-accessible surface area (ΔASA) (*64*). Small perturbations, such as single point mutations, are not expected to change them significantly, unless they strongly disrupt the native, intermediate, or unfolded conformations. Native apo- and PLP-eAATases (E. Deu and J. F. Kirsch, accompanying paper, and Figure 3) exhibit identical CD spectra, and D* is a common intermediate. Thus, no large structural perturbation is effected by association of the cofactor to the apoenzyme. Additionally, $m_{D\rightleftarrows D^*}$ values obtained for the PMP form (Table 3) and holo-eAATase mutants that do not show overlapping denaturation transitions (E. Deu and J. F. Kirsch, unpublished data) are within experimental error of that of the apo form. Approximate ΔG^0 values for the PLP form were therefore obtained by fixing the *m* values to those of the apo form in the global fitting of the data.

Only the data obtained at 10 μM enzyme were fitted for the PMP form since no overlap between the two denaturation transitions was observed at that concentration (Figure 6). The thermodynamic parameters obtained for both holo forms are reported in Table 3. The difference in free energy of association between the two cofactors calculated from their dissociation constants (*23*) ($K_{D,PLP}$ = 0.4 pM and $K_{D,PMP}$ = 1.3 nM) is 4.8 kcal mol^{-1}. This value is equal to the difference in $\Delta G^0_{D\rightleftarrows D^*}$ values (Table 3) between the PLP and PMP forms, although the propagated error in the subtraction (3.2 kcal mol^{-1}) is large.

(*B) Reduced Form.* The D-PPL_2 ⇄ 2M′-PPL transition is not accompanied by a fluorescence emission signal. Therefore, $\Delta G^0_{M'-PPL\rightleftarrows U-PPL}$ can be obtained by fitting the emission data (Figure 7 insets) to eq 5, with $K_{M'-PPL\rightleftarrows U-PPL} = \exp[-(\Delta G^0_{M'-PPL\rightleftarrows U-PPL} - m_{M'-PPL\rightleftarrows U-PPL}[\text{urea}])/RT]$. $\Delta G^0_{D-PPL_2\rightleftarrows 2M'-PPL}$ was evaluated from the CD data. The mole fractions of the monomer intermediate ($X_{M'-PPL}$) were calculated with eq 12 at those urea and enzyme concentrations where D-PPL_2 and M′-PPL are the only significantly populated species. Their associated $\Delta G_{D-PPL2\rightleftarrows 2M'-PPL}$ values were obtained with eq 13 (E. Deu and J. F. Kirsch, accompanying paper), and $\Delta G^0_{D-PPL_2\rightleftarrows 2M'-PPL}$ was extrapolated to 0 M denaturant according to eq 14 (Table 3, Figure 9).

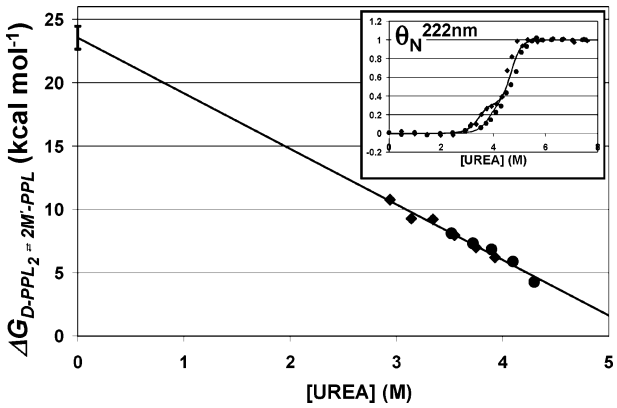

FIGURE 9: Evaluation of the free energy of dissociation of D-PPL_2 to 2M′-PPL by linear extrapolation. The $\Delta G_{D-PPL_2\rightleftarrows 2M'-PPL}$ values at each urea and enzyme concentration were computed (eqs 12 and 13) from the CD data collected at 0.5 (◆) and 10 μM (●) PPL-eAATase and fitted to eq 14 (solid line). The values of the determined parameters are reported in Table 3. The inset shows the simulated PPL-eAATase denaturation curves obtained from the stability parameters in Table 3 for the CD data of Figure 7.

$$X_{M'-PPL} = \frac{[\text{M}'\text{-PPL}]}{P_T} = \frac{S - (S^0_D + \alpha_D[\text{urea}])}{(S^0_{M'-PPL} + \alpha_{M'-PPL}[\text{urea}]) - (S^0_D + \alpha_D[\text{urea}])} \quad (12)$$

$$\Delta G_{D-PPL_2\rightleftarrows 2M'-PPL} = -RT \ln\left(\frac{2P_T X_{M'-PPL}^2}{1 - X_{M'-PPL}}\right) \quad (13)$$

$$\Delta G_{D-PPL_2\rightleftarrows 2M'-PPL} = \Delta G^0_{D-PPL_2\rightleftarrows 2M'-PPL} - m_{D-PPL_2\rightleftarrows 2M'-PPL}[\text{urea}] \quad (14)$$

P_T is the total monomer concentration; $X_{M'-PPL}$, the mole fraction of M′-PPL; and S_i^0 and α_i are defined in eq 5. The validity of this approach was tested by simulation of the PPL-form CD denaturation curves from the thermodynamic parameters reported in Table 3 (Figure 9 inset).

Global Stability Model for eAATase. In all eAATase variants, the presence of two structural regions with distinct stabilities is indicated by two cooperative denaturation transitions. These are the active site region (ASR), whose stability increases in the presence of cofactor (Figures 8 and 10), and the dimerization region (DMR). The DMR contains the intersubunit interactions that stabilize D*. Those might also be key interface contacts in the native state. Its stability is unaffected by either PMP or PLP; therefore, the region must be removed from the active site. The DMR is more stable than the ASR in all eAATase variants, except that of the PPL form.

The thermodynamic parameters of Table 3 can be misleading because they indicate that the PPL-form ASR ($\Delta G^0_{M'-PPL\rightleftarrows U}$ = 14.5 kcal mol^{-1}) is less stable than the DMR ($\Delta G^0_{D-PPL2\rightleftarrows 2M'-PPL}$ = 23.5 kcal mol^{-1}). However, those values are calculated for a 1 M standard state, which is not representative of the experimental conditions. Figure 10

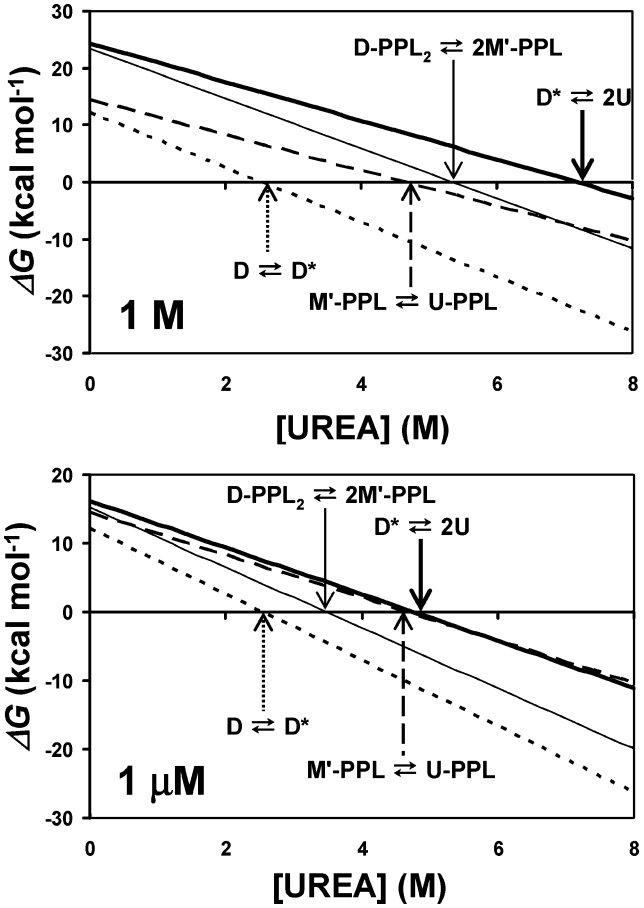

FIGURE 10: Denaturation equilibria dependencies of the apo and PPL forms of eAATase on urea concentration. The free energies of unfolding of the DMR (solid lines) and ASR (discontinuous lines) were calculated at 1 M and 1 μM standard states and are shown in the upper and lower panels, respectively. The arrows indicate the denaturant concentrations at which the labeled transitions become thermodynamically favored ($\Delta G < 0$ kcal mol^{-1}). The downward arrows point at dimer dissociation processes, whose associated ΔG's are decreased by more than 8 kcal mol^{-1} between the 1 M and 1 μM standard states: D* ⇄ 2U (thick lines) and D-PPL$_2$ ⇄ 2M′-PPL (thin lines). The apo form D ⇄ D* (dotted line) and the PPL form M′-PPL ⇄ U-PPL (dashed line) transitions are protein concentration independent, and their ΔG values are the same in both panels. The order in which the unimolecular and dissociation reactions become favored is inverted between the two standard states for PPL-eAATase.

illustrates the urea dependence of the free energies of unfolding for the apo and PPL forms at 1 M and 1 μM standard states. Denaturation of the PPL-form ASR would occur at lower urea concentrations than the dissociation process were the protein concentration 1 M (Figure 10, upper panel). However, free energies calculated at a more representative standard state (1 μM) are in agreement with the experimental results; i.e., the DMR disorders at lower urea concentrations than does the ASR.

As the number and/or strength of the cofactor/active site interactions increase(s) serially, from apo- to the PMP, PLP, and PPL forms, the stability of the ASR strengthens to the point where the relative stabilities of the ASR and DMR become reversed. This model, illustrated in Scheme 1, explains the formation of a monomeric rather than a dimeric intermediate for PPL-eAATase. The ASR might be larger than the DMR as 60% of the secondary structure is lost in the D ⇄ D* transition (denaturation of the ASR). Further,

Scheme 1: Model for eAATase Denaturation in Urea[a]

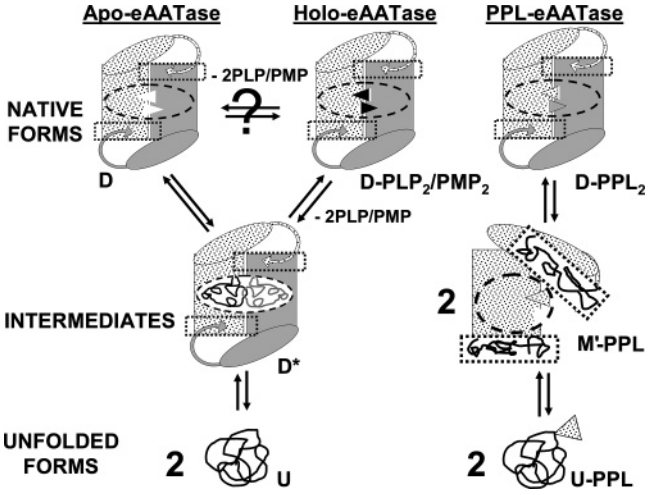

[a] The filled and dotted areas each represent one of the two homodimer subunits. Vacant and cofactor-occupied active sites are shown by open and closed triangles, respectively. The areas enclosed in the dashed and dotted lines refer to the two structural regions described in the text: ASR (oval) and DMR (rectangles). Their losses of structure are indicated by random coils. The ASR is less stable in the apo form, yielding a stable dimeric intermediate (D*). The holoenzyme may convert to D* concomitantly with cofactor release, or the pyridoxyl moiety may dissociate first, generating D. The relative stabilities of the two regions are inverted in the reduced form due to stabilization of the ASR by PPL. The DMR unfolds first, yielding M′-PPL, which retains a largely intact ASR.

the 30% loss of secondary structure observed for the PPL form upon M′-PPL formation is consistent with the unfolding of the smaller DMR.

The ASR and DMR might correspond physically to the large and small domains of eAATase, respectively. The former contains the active sites, and the latter has an N-terminal tail that wraps around the opposite subunit. None of eAATase tryptophan residues is situated in the small domain, which might explain why no change in fluorescence emission is observed in the D-PPL$_2$ ⇄ 2M′-PPL transition. Additionally, deletion of the small domain yields a monomeric folded protein (*65*), thus indicating that the interactions across large domains (ASR) are not sufficient to form a dimer.

ACKNOWLEDGMENT

We thank Dr. Keith A. Koch for the cloning of His$_6$-tagged eAATase and Dr. Katie Tripp for thoughtful comments and helpful suggestions on the manuscript.

REFERENCES

1. Wittung-Stafshede, P. (2002) Role of cofactors in protein folding, *Acc. Chem. Res. 35*, 201−208.
2. Wardell, S. E., Kwok, S. C., Sherman, L., Hodges, R. S., and Edwards, D. P. (2005) Regulation of the amino-terminal transcription activation domain of progesterone receptor by a cofactor-induced protein folding mechanism, *Mol. Cell. Biol. 25*, 8792−8808.
3. Muralidhara, B. K., and Wittung-Stafshede, P. (2005) FMN binding and unfolding of *Desulfovibrio desulfuricans* flavodoxin: "hidden" intermediates at low denaturant concentrations, *Biochim. Biophys. Acta 1747*, 239−250.
4. Bollen, Y. J., Nabuurs, S. M., van Berkel, W. J., and van Mierlo, C. P. (2005) Last in, first out: the role of cofactor binding in flavodoxin folding, *J. Biol. Chem. 280*, 7836−7844.

5. Wittung-Stafshede, P. (2004) Role of cofactors in folding of the blue-copper protein azurin, *Inorg. Chem. 43*, 7926−7933.
6. Oses-Prieto, J. A., Bengoechea-Alonso, M. T., Artigues, A., Iriarte, A., and Martinez-Carrion, M. (2003) The nature of the rate-limiting steps in the refolding of the cofactor-dependent protein aspartate aminotransferase, *J. Biol. Chem. 278*, 49988−49999.
7. Apiyo, D., and Wittung-Stafshede, P. (2002) Presence of the cofactor speeds up folding of *Desulfovibrio desulfuricans* flavodoxin, *Protein Sci. 11*, 1129−1135.
8. Muralidhara, B. K., Rathinakumar, R., and Wittung-Stafshede, P. (2006) Folding of *Desulfovibrio desulfuricans* flavodoxin is accelerated by cofactor fly-casting, *Arch. Biochem. Biophys. 451*, 51−58.
9. Pant, K., and Crane, B. R. (2005) Structure of a loose dimer: an intermediate in nitric oxide synthase assembly, *J. Mol. Biol. 352*, 932−940.
10. Jaenicke, R. (1999) Stability and folding of domain proteins, *Prog. Biophys. Mol. Biol. 71*, 155−241.
11. Noland, B. W., and Baldwin, T. O. (2003) Demonstration of two independently folding domains in the alpha subunit of bacterial luciferase by preferential ligand binding-induced stabilization, *Biochemistry 42*, 3105−3112.
12. Flaugh, S. L., Kosinski-Collins, M. S., and King, J. (2005) Contributions of hydrophobic domain interface interactions to the folding and stability of human gammaD-crystallin, *Protein Sci. 14*, 569−581.
13. Ahmad, B., Ahmed, M. Z., Haq, S. K., and Khan, R. H. (2005) Guanidine hydrochloride denaturation of human serum albumin originates by local unfolding of some stable loops in domain III, *Biochim. Biophys. Acta 1750*, 93−102.
14. Herold, M., and Kirschner, K. (1990) Reversible dissociation and unfolding of aspartate aminotransferase from *Escherichia coli*: characterization of a monomeric intermediate, *Biochemistry 29*, 1907−1913.
15. Leistler, B., Herold, M., and Kirschner, K. (1992) Collapsed intermediates in the reconstitution of dimeric aspartate aminotransferase from *Escherichia coli*, *Eur. J. Biochem. 205*, 603−611.
16. Birolo, L., Malashkevich, V. N., Capitani, G., De Luca, F., Moretta, A., Jansonius, J. N., and Marino, G. (1999) Functional and structural analysis of cis-proline mutants of *Escherichia coli* aspartate aminotransferase, *Biochemistry 38*, 905−913.
17. Birolo, L., Dal Piaz, F., Pucci, P., and Marino, G. (2002) Structural characterization of the M* partly folded intermediate of wild type and P138A aspartate aminotransferase from *Escherichia coli*, *J. Biol. Chem. 277*, 17428−17437.
18. Reyes, A. M., Iriarte, A., and Martinez-Carrion, M. (1993) Refolding of the precursor and mature forms of mitochondrial aspartate aminotransferase after guanidine hydrochloride denaturation, *J. Biol. Chem. 268*, 22281−22291.
19. Artigues, A., Iriarte, A., and Martinez-Carrion, M. (1994) Acid-induced reversible unfolding of mitochondrial aspartate aminotransferase, *J. Biol. Chem. 269*, 21990−21999.
20. Relimpio, A., Iriarte, A., Chlebowski, J. F., and Martinez-Carrion, M. (1981) Differential scanning calorimetry of cytoplasmic aspartate transaminase, *J. Biol. Chem. 256*, 4478−4488.
21. Velick, S. F., and Vavra, J. (1962) A kinetic and equilibrium analysis of the glutamic oxaloacetate transaminase mechanism, *J. Biol. Chem. 237*, 2109−2122.
22. Kirsch, J. F., Eichele, G., Ford, G. C., Vincent, M. G., Jansonius, J. N., Gehring, H., and Christen, P. (1984) Mechanism of action of aspartate aminotransferase proposed on the basis of its spatial structure, *J. Mol. Biol. 174*, 497−525.
23. Toney, M. D., and Kirsch, J. F. (1991) Kinetics and equilibria for the reactions of coenzymes with wild type and the Y70F mutant of *Escherichia coli* aspartate aminotransferase, *Biochemistry 30*, 7461−7466.
24. Jager, J., Moser, M., Sauder, U., and Jansonius, J. N. (1994) Crystal structures of *Escherichia coli* aspartate aminotransferase in two conformations. Comparison of an unliganded open and two liganded closed forms, *J. Mol. Biol. 239*, 285−305.
25. Jager, J., Pauptit, R. A., Sauder, U., and Jansonius, J. N. (1994) Three-dimensional structure of a mutant *E. coli* aspartate aminotransferase with increased enzymic activity, *Protein Eng. 7*, 605−612.
26. Okamoto, A., Higuchi, T., Hirotsu, K., Kuramitsu, S., and Kagamiyama, H. (1994) X-ray crystallographic study of pyridoxal 5′-phosphate-type aspartate aminotransferases from *Escherichia coli* in open and closed form, *J. Biochem. (Tokyo) 116*, 95−107.
27. Miyahara, I., Hirotsu, K., Hayashi, H., and Kagamiyama, H. (1994) X-ray crystallographic study of pyridoxamine 5′-phosphate-type aspartate aminotransferases from *Escherichia coli* in three forms, *J. Biochem. (Tokyo) 116*, 1001−1012.
28. Toney, M. D., and Kirsch, J. F. (1991) Tyrosine 70 fine-tunes the catalytic efficiency of aspartate aminotransferase, *Biochemistry 30*, 7456−7461.
29. Toney, M. D., and Kirsch, J. F. (1993) Lysine 258 in aspartate aminotransferase: enforcer of the Circe effect for amino acid substrates and general-base catalyst for the 1,3-prototropic shift, *Biochemistry 32*, 1471−1479.
30. Kochhar, S., Finlayson, W. L., Kirsch, J. F., and Christen, P. (1987) The stereospecific labilization of the C-4′ pro-S hydrogen of pyridoxamine 5′-phosphate is abolished in (Lys258→Ala) aspartate aminotransferase, *J. Biol. Chem. 262*, 11446−11448.
31. Kuramitsu, S., Inoue, Y., Tanase, S., Morino, Y., and Kagamiyama, H. (1987) Substitution of an arginyl residue for the active site lysyl residue (Lys258) of aspartate aminotransferase, *Biochem. Biophys. Res. Commun. 146*, 416−421.
32. Malcolm, B. A., and Kirsch, J. F. (1985) Site-directed mutagenesis of aspartate aminotransferase from *E. coli*, *Biochem. Biophys. Res. Commun. 132*, 915−921.
33. Toney, M. D., and Kirsch, J. F. (1987) Tyrosine 70 increases the coenzyme affinity of aspartate aminotransferase. A site-directed mutagenesis study, *J. Biol. Chem. 262*, 12403−12405.
34. Toney, M. D., and Kirsch, J. F. (1989) Direct Bronsted analysis of the restoration of activity to a mutant enzyme by exogenous amines, *Science 243*, 1485−1488.
35. Toney, M. D., and Kirsch, J. F. (1991) The K258R mutant of aspartate aminotransferase stabilizes the quinonoid intermediate, *J. Biol. Chem. 266*, 23900−23903.
36. Toney, M. D., and Kirsch, J. F. (1992) Bronsted analysis of aspartate aminotransferase via exogenous catalysis of reactions of an inactive mutant, *Protein Sci. 1*, 107−119.
37. Planas, A., and Kirsch, J. F. (1991) Reengineering the catalytic lysine of aspartate aminotransferase by chemical elaboration of a genetically introduced cysteine, *Biochemistry 30*, 8268−8276.
38. Gloss, L. M., and Kirsch, J. F. (1995) Examining the structural and chemical flexibility of the active site base, Lys-258, of *Escherichia coli* aspartate aminotransferase by replacement with unnatural amino acids, *Biochemistry 34*, 12323−12332.
39. Gloss, L. M., and Kirsch, J. F. (1995) Decreasing the basicity of the active site base, Lys-258, of *Escherichia coli* aspartate aminotransferase by replacement with gamma-thialysine, *Biochemistry 34*, 3990−3998.
40. Ziak, M., Jaussi, R., Gehring, H., and Christen, P. (1990) Aspartate aminotransferase with the pyridoxal-5′-phosphate-binding lysine residue replaced by histidine retains partial catalytic competence, *Eur. J. Biochem. 187*, 329−333.
41. Inoue, K., Kuramitsu, S., Okamoto, A., Hirotsu, K., Higuchi, T., and Kagamiyama, H. (1991) Site-directed mutagenesis of *Escherichia coli* aspartate aminotransferase: role of Tyr70 in the catalytic processes, *Biochemistry 30*, 7796−7801.
42. Birolo, L., Sandmeier, E., Christen, P., and John, R. A. (1995) The roles of Tyr70 and Tyr225 in aspartate aminotransferase assessed by analysing the effects of mutations on the multiple reactions of the substrate analogue serine o-sulphate, *Eur. J. Biochem. 232*, 859−864.
43. Yano, T., Mizuno, T., and Kagamiyama, H. (1993) A hydrogen-bonding network modulating enzyme function: asparagine-194 and tyrosine-225 of *Escherichia coli* aspartate aminotransferase, *Biochemistry 32*, 1810−1815.
44. Goldberg, J. M., Swanson, R. V., Goodman, H. S., and Kirsch, J. F. (1991) The tyrosine-225 to phenylalanine mutation of *Escherichia coli* aspartate aminotransferase results in an alkaline transition in the spectrophotometric and kinetic pK_a values and reduced values of both k_{cat} and K_m, *Biochemistry 30*, 305−312.
45. Goldberg, J. M., Zheng, J., Deng, H., Chen, Y. Q., Callender, R., and Kirsch, J. F. (1993) Structure of the complex between pyridoxal 5′-phosphate and the tyrosine 225 to phenylalanine mutant of *Escherichia coli* aspartate aminotransferase determined by isotope-edited classical Raman difference spectroscopy, *Biochemistry 32*, 8092−8097.
46. Goldberg, J. M., and Kirsch, J. F. (1996) The reaction catalyzed by *Escherichia coli* aspartate aminotransferase has multiple partially rate-determining steps, while that catalyzed by the Y225F mutant is dominated by ketimine hydrolysis, *Biochemistry 35*, 5280−5291.

47. Park, Y., Luo, J., Schultz, P. G., and Kirsch, J. F. (1997) Noncoded amino acid replacement probes of the aspartate aminotransferase mechanism, *Biochemistry 36*, 10517−10525.
48. Yano, T., Kuramitsu, S., Tanase, S., Morino, Y., and Kagamiyama, H. (1992) Role of Asp222 in the catalytic mechanism of *Escherichia coli* aspartate aminotransferase: the amino acid residue which enhances the function of the enzyme-bound coenzyme pyridoxal 5′-phosphate, *Biochemistry 31*, 5878−5887.
49. Onuffer, J. J., and Kirsch, J. F. (1994) Characterization of the apparent negative co-operativity induced in *Escherichia coli* aspartate aminotransferase by the replacement of Asp222 with alanine. Evidence for an extremely slow conformational change, *Protein Eng. 7*, 413−424.
50. Hayashi, H., Inoue, Y., Kuramitsu, S., Morino, Y., and Kagamiyama, H. (1990) Effects of replacement of tryptophan-140 by phenylalanine or glycine on the function of *Escherichia coli* aspartate aminotransferase, *Biochem. Biophys. Res. Commun. 167*, 407−412.
51. Deu, E., Koch, K. A., and Kirsch, J. F. (2002) The role of the conserved Lys68*:Glu265 intersubunit salt bridge in aspartate aminotransferase kinetics: multiple forced covariant amino acid substitutions in natural variants, *Protein Sci. 11*, 1062−1073.
52. Cronin, C. N., and Kirsch, J. F. (1988) Role of arginine-292 in the substrate specificity of aspartate aminotransferase as examined by site-directed mutagenesis, *Biochemistry 27*, 4572−4579.
53. Kempe, T. D., and Stark, G. R. (1975) Pyridoxal 5′-phosphate, a fluorescent probe in the active site of aspartate transcarbamylase, *J. Biol. Chem. 250*, 6861−6869.
54. Pace, C. N. (1986) Determination and analysis of urea and guanidine hydrochloride denaturation curves, *Methods Enzymol. 131*, 266−280.
55. Pace, C. N., and Shaw, K. L. (2000) Linear extrapolation method of analyzing solvent denaturation curves, *Proteins* (Suppl. 4), 1−7.
56. Santoro, M. M., and Bolen, D. W. (1988) Unfolding free energy changes determined by the linear extrapolation method. 1. Unfolding of phenylmethanesulfonyl alpha-chymotrypsin using different denaturants, *Biochemistry 27*, 8063−8068.
57. Noland, B. W., Dangott, L. J., and Baldwin, T. O. (1999) Folding, stability, and physical properties of the alpha subunit of bacterial luciferase, *Biochemistry 38*, 16136−16145.
58. Barrick, D., and Baldwin, R. L. (1993) Three-state analysis of sperm whale apomyoglobin folding, *Biochemistry 32*, 3790−3796.
59. Gloss, L. M., Planas, A., and Kirsch, J. F. (1992) Contribution to catalysis and stability of the five cysteines in *Escherichia coli* aspartate aminotransferase. Preparation and properties of a cysteine-free enzyme, *Biochemistry 31*, 32−39.
60. Sinclair, J. F., Ziegler, M. M., and Baldwin, T. O. (1994) Kinetic partitioning during protein folding yields multiple native states, *Nat. Struct. Biol. 1*, 320−326.
61. Lai, Z., McCulloch, J., Lashuel, H. A., and Kelly, J. W. (1997) Guanidine hydrochloride-induced denaturation and refolding of transthyretin exhibits a marked hysteresis: equilibria with high kinetic barriers, *Biochemistry 36*, 10230−10239.
62. Fasshauer, D., Antonin, W., Subramaniam, V., and Jahn, R. (2002) SNARE assembly and disassembly exhibit a pronounced hysteresis, *Nat. Struct. Biol. 9*, 144−151.
63. Engel, J., and Bachinger, H. P. (2000) Cooperative equilibrium transitions coupled with a slow annealing step explain the sharpness and hysteresis of collagen folding, *Matrix Biol. 19*, 235−244.
64. Myers, J. K., Pace, C. N., and Scholtz, J. M. (1995) Denaturant m values and heat capacity changes: relation to changes in accessible surface areas of protein unfolding, *Protein Sci. 4*, 2138−2148.
65. Herold, M., Leistler, B., Hage, A., Luger, K., and Kirschner, K. (1991) Autonomous folding and coenzyme binding of the excised pyridoxal 5′-phosphate binding domain of aspartate aminotransferase from *Escherichia coli*, *Biochemistry 30*, 3612−3620.

BI602632D